

ATOMIC MOBILITY IN TITANIUM GRADE 5 (Ti6Al4V)

W. Gierlotka ^a, G. Lothongkum ^b, B. Lohwongwatana ^b, C. Puncreoburt ^b^aMaterials Science and Engineering Department, National Taiwan University, Taiwan, R.O.C.^bDepartment of Metallurgical Engineering, Chulalongkorn University, Thailand

(Received 20 June 2018; accepted 29 November 2018)

Abstract

Titanium grade 5 (Ti6Al4V) is a modern material that can be found in a wide spectrum of applications, from medicine to aircraft industry. The commercial alloy is a mix of a body centered cubic structure (BCC_A2) and a hexagonal closed packed structure (HCP_A3). It is obvious, that heat treatment of the alloy will change a ratio between BCC_A2 and HCP_A3 and, as a consequence, properties of a material. Information about mobility of atoms in both crystal structures allows simulations and predictions of structures' behavior during the heat treatment and diffusion. In this work the atomic mobility in liquid, BCC_A2, and HCP_A3 phases of ternary alloy Al – Ti – V were obtained based on available literature information. Comparison between simulations and experiments shows a good agreement, hence it can be concluded that proposed set of kinetic parameters can be used for predictions and simulations of Titanium grade 5 heat treatment.

Keywords: Titanium; Kinetic modeling; DICTRA.

1. Introduction

In recent years titanium and its alloys started to play important role in wide range of applications due to their excellent properties, such as strength or corrosion resistance [1]. The workhorse among titanium alloys is Ti6Al4V, also known as Titanium grade 5. This particular alloy had been used in aerospace industry, chemical industry, as a biomaterial and so on because of its outstanding physico-chemical properties [2]. Casting of the Ti6Al4V alloy gives a mix of grains with structure of Ti- α (HCP_A3) and Ti- β (BCC_A2), therefore a heat treatment is a way for steering the ratio of both kind of crystals. Similarly, cooling rate of solidification plays important role in the produced structure. In both cases a knowledge of atoms mobility allows the prediction and more precise guiding of a heat treatment or casting process. Therefore, it appears that a kinetic description of atoms in Ti-rich corner of the ternary Al – Ti – V system is a necessary tool for industry. To the best knowledge of authors a consistent description of Ti, Al, and V mobility in Ti-rich BCC_A2, HCP_A3, and liquid phases has not been published yet, hence the purpose of this study was to prepare a kinetic description of above mentioned elements in Ti- α , Ti- β , and liquid phases based on experimental data and theoretical models.

2. Theoretical background

Fick's 2nd law in the mass conservative form (1) gives the temporal profile of the diffusing specie k.

$$\frac{\partial C_k}{\partial t} = -V_m \text{div}(J_k) \quad (1)$$

Where t is time [s] C_k is the concentration in [mol m⁻³], V_m is a molar volume [m³ mol⁻¹] and J_k is the diffusional flux [mol m⁻² s⁻¹] given by:

$$J_k = -\sum_{j=1}^{n-1} D_{kj}^n \nabla C_j \quad (2)$$

The chemical diffusion coefficient D_{kj}^n [m² s⁻¹] which summation is performed over (n-1) independent concentrations as the dependent n-th component can be taken as the solvent, k, j denote independent components. For a substitution solution, the diffusion coefficient can be expressed as:

$$D_{kj}^n = \sum_i (\delta_{ik} - x_k) x_i M_i \left(\frac{\partial \mu_i}{\partial x_j} - \frac{\partial \mu_i}{\partial x_n} \right) \quad (3)$$

Where δ_{ik} is Kronecker's delta, x_i , m_i , M_i are the mole fraction, chemical potential [J mol⁻¹] and atomic mobility [m² J⁻¹ s⁻¹] of the i-th component, respectively.

The mobility parameter M_i can be divided into frequency parameter M_i^0 [m² J⁻¹ s⁻¹] and activation energy Q_i [J mol⁻¹]

*Corresponding author: wojtek@gms.ndhu.edu.tw



$$M_i = \exp\left(\frac{RT \ln(M_i^0)}{RT}\right) \exp\left(\frac{-Q_i}{RT}\right) \frac{1}{RT} {}^{mg}\Omega \quad (4)$$

where ${}^{mg}\Omega$ is a factor depending on magnetic contribution to the diffusion, R , T are universal gas constant [J mol⁻¹ K⁻¹] and absolute temperature [K], respectively. It is possible to rewrite Eq. 4 in a form:

$$M_i = \exp\left(\frac{\Delta G_i^\phi}{RT}\right) \frac{1}{RT} {}^{mg}\Omega \quad (5)$$

where

$$\Delta G_i^\phi = RT \ln(M_i^0) - Q_i \quad (6)$$

is a parameter. The superscript ϕ suggests connection between ΔG_i^ϕ and frequency parameter [J mol⁻¹].

Anderson and Agren [3] suggested that the ΔG_i^ϕ should be a function of the composition given by Redlich – Kister [4] polynomial, which is in agreement with the CALPHAD method. For the binary substitutional solution without magnetic influence the expression has the following form:

$$\Delta G^\phi = x_m \Delta G_i^m + x_n \Delta G_i^n + x_m x_n \sum_i \Delta^{(j)} G_i^{m,n} (x_m - x_n) \quad (7)$$

Where ΔG_i^m , ΔG_i^n , $\Delta^{(j)} G_i^{m,n}$ are values of ΔG^ϕ for pure elements m and n and an interaction parameter for diffusion between m and n , respectively.

Using Einstein's equation and assuming a non-vacancy atomic exchange as the main diffusion mechanism, the tracer diffusivity D_i^* [m² s⁻¹] is related to atomic mobility:

$$D_i^* = RTM_i \quad (8)$$

For the binary m-n system, the chemical diffusion coefficient can be calculated from tracer diffusivity [m² s⁻¹]:

$$\tilde{D} = (x_m D_m^* + x_n D_n^*) \phi \quad (9)$$

Where the thermodynamic factor is given as follows:

$$\phi = 1 + \frac{d \ln(\gamma_m)}{d \ln(x_m)} = \frac{x_m}{RT} \frac{\partial \mu_m}{\partial x_m} = \frac{x_m(1-x_m)}{RT} \frac{dG}{dx_m^2} \quad (10)$$

where G is Gibbs energy of the phase [J mol⁻¹], Y_m is the activity coefficient of component m .

In the case of the ternary Al – Ti – V system there are hypothetical BCC_A2 and HCP_A3 lattice for Al and Al, Ti, respectively. The self-diffusivity of these elements in the hypothetical crystal lattice is calculated based on the empirical relation given by Leclair [5]:

$$Q_i = RT^f (K + 1.5V) \quad (11)$$

and by Askil [6]:

$$M_i^0 = 1.04 \times 10^{-3} Q_i a^2 \quad (12)$$

where K is a structure factor equal 15.5 for a HCP_A3 phase, and equal 13 for BCC_A2 structure, V is the valence and a is the lattice constant [nm] and T^f is melting temperature [K]. The impurity diffusion coefficients in hypothetical Al BCC_A as well as Al HCP_A3 and V HCP_A3 were obtained from Du et al. [7] approach given by Equation 13 and 14:

$$\ln(D_A^{0A} \times D_B^{0B}) = \ln(D_B^{0A} \times D_A^{0B}) \quad (13)$$

$$Q_A^A + Q_B^B = Q_A^B + Q_B^A \quad (14)$$

where D_A^{0A} , D_B^{0B} are self-diffusion coefficients of elements A and B, respectively, D_A^{0A} , D_B^{0B} are impurity diffusion coefficients, Q_A^A , Q_B^B , Q_A^B , Q_B^A are activation energies. In a case of liquid phase with no experimental data, the self-diffusion was calculated following Fredriksson and Akerlind [8]:

$$D_n^{n,liquid} = 0.35 \times 10^{-9} \left(\frac{T^f}{M}\right)^{\frac{1}{2}} V^{\frac{1}{3}} \quad (15)$$

where M is a molar mass [kg], V is a molar volume [m³ mol⁻¹].

3. Literature review

Since the diffusion is a property that is usually determined experimentally, the literature information used for modeling is crucial. Diffusion of Ti and V in BCC_A2 phase in binary system Ti – V was determined in a wide temperature range and in a full composition range due to continuous solid solution, which is formed at high temperature between titanium and vanadium in body centered cubic structure. The self-diffusion and inter-diffusion of zirconium, molybdenum, vanadium, and oxygen in the temperature range 873 K – 1573 K was reported by Elliot [9] who used radioactive titanium and diffusion couple methods. Murdock et al. [10] determined self-diffusion coefficient of Ti and impurity-diffusion coefficient of V in Ti BCC_A2 at temperature range between 1173 K and 1823 K. The self-diffusion of Ti in body centered cubic structure was also determined by Gerold and Herzig [11] at temperature range 1607 K – 1829 K, and by Walsoe et al. [12] at 1173 – 1853 K. The interdiffusion coefficients in binary Ti-V BCC_A2 system were measured by Murdock et al. [13] and by Ugaste et al. [14] at temperature range 1473 K – 1873 K, and 1273 K – 1673K, respectively. Both papers [13,14] reported the experimental values of interdiffusion coefficients for whole composition range of binary Ti – V system. The self-diffusion of vanadium in BCC_A2 structure was measured by Pelleg [15] at temperatures between 997 K and 2115 K, George et al. [16] at 1323 K – 2147 K, and by Macht et al. [17] and by Agarwala et al. [18] who determined the self-diffusion coefficient at temperature ranges 1443 K –

2166 K, and 973 K – 1673 K, respectively. All the works [15-18] used a radioactive V^{48} tracer in pure V crystals. The impurity diffusion of Ti in BCC_A2 V was determined by Murdock et al. [13] at temperature range 1473 K – 1873 K. Due to the very small solubility of vanadium in titanium HCP_A3 the experimental data of interdiffusion in this phase is limited. To the best of author's knowledge, only Elliot [9] reported interdiffusion coefficient in binary Ti-V HCP_A3 at 873 K and 973 K. The self-diffusion of Ti in HCP_A3 structure was reported by Elliot [9], and Perez et al. [19] at temperature range 873 K – 1073 K, and it was calculated by ab-initio method by Scotti and Mottura [20] at temperature range 873 – 1133 K as well. It has to be pointed out, that Scotti and Mottura [20] determined the diffusion coefficient for perpendicular and parallel directions to basal plane of hexagonal close-packed structure. Following Perez et al., the average diffusion in HCP_A3 structure can be taken as:

$$D_{\alpha} = (2D_{\perp} + D_{\parallel})/3 \quad (16)$$

The impurity diffusion of V in Ti HCP_A3 was determined from first principle calculation by Xu et al. [21].

The impurity diffusion of Al in BCC_A2 titanium was measured by Koppers et al. [22] at temperature range between 1173 and 1813 K, by Araki et al. [23] at 1173 K - 1673 K, and by Lee et al. [24] at 1323 K – 1823 K. The interdiffusion coefficient of binary Al – Ti body centered cubic phase was determined by Lee et al. [24] at temperature range 1323 K – 1823 K for composition range $x_{Al} = 0.2$ to $x_{Al} = 0.12$. Araki [23] measured the interdiffusion coefficient at 1173 K - 1673 K and composition range of aluminum between 0.045 and 0.145 mole fraction. The impurity diffusion coefficient Al in Ti HCP_A3 was measured by Koppers et al. [25] at temperature range 950 K – 1150 K by aid of penetration profiles as well as Raisen et al. [26] by residual activity method, and by Mishin and Herzig [27]. There is no experimental data about interdiffusion coefficient in binary Al – Ti HCP_A3 phase at low temperature. The high temperature, high Al concentration interdiffusion was studied at 1442 K, 1542 K, and at 1591 K by Kainuma and Inden [28]; however, due to temperature of the experiment that is much higher than experimental information about self and impurity diffusion in Ti HCP_A3, the data was not used in the present calculation. The impurity diffusion of Al in HCP_A3 Ti was calculated by Lu et al. [29]. Kinetic modeling of BCC_A2 phase in the Ti -V system was done by Liu et al. [30]. The modeling of atomic mobility in Al – Ti was proposed by Chen et al. [31] in their work on Ti-Al-Fe system. The information about ternary diffusion in Ti-rich alloys of Al – Ti – V system is very limited. Takahashi et al. [32] determined interdiffusion in Ti BCC_A2

phase by aid of concentration profile method at 1373 K and at 1473 K. Moreover, Siemiatin et al. [33] proposed diffusion coefficients for particular Ti-6Al-4V alloy based on experiment done at 1227 K, 1172 K, and at 1116 K.

4. Calculation procedure

All the kinetic calculations were done using Thermocalc package [34] with Parrot module. The thermodynamic database of liquid, BCC_A2, and HCP_A3 phases was retrieved from Lu et al. [29] thermodynamic description of the ternary Al – Ti – V system. After that, mobility parameters were added to the description in the DICTRA module of Thermocalc [34] in a form of adjustable variables. Most of the variables were optimized using available experimental data. Kinetic parameters obtained in this work, along with thermodynamic parameters taken from literature [29], are gathered in Tables 1 and 2.

It has to be mentioned here, that thermodynamic parameters [10] used in this work generate inverted miscibility gaps at high temperature for the binary Al – Ti system. In order to avoid this kind of problem it was decided to re-optimize the liquid phase of Al – Ti system. Details of this re-optimization are given in Appendix 1.

5. Results and discussion

Although the description of binary mobility in BCC_A2 phase was already proposed [29,31] it was decided to re-optimize the binary parameters for BCC_A2 phase to keep whole description consistent. The self-diffusion of Ti BCC_A2 and HCP_A3 is shown in Figure 1 along with experimental data given by Elliot [9], Walsoe et al. [12], Murdock et al. [10], Gerold and Herzig [11], Perez et al. [19], and Scotti and Moutura [20].

It is obvious that experimental determination of self-diffusion of Ti in body centered cubic are self-consistent and calculation follows the data faultless. Different situation can be seen by looking at experimental determination of self-diffusion of Ti in HCP structure. In this case the data is not consistent and all three sources provide different information. Self-diffusion of Ti in hexagonal structure reported by Elliot [9] shows opposite temperature trend from data given by Perez et al. [19] and Scotti and Moutura [20], therefore Elliot's [9] data was not considered as an information used for optimization. The experimental results given by Perez et al. [19] and Scotti and Moutura [20] exhibit the same temperature dependency but show different activation energy. Since Perez et al. [19] didn't provide information about crystallographic directions of measured diffusion, their data had lower weight during



Table 1. Mobility parameters in Titanium grade 5 obtained in this work

Phase	Element	Mobility
BCC_A2	Al	$MQ(BCC_A2, Al;0) = -110721-266.41*T$
		$MQ(BCC_A2, Ti;0) = -159367.966-125.405247*T$
		$MQ(BCC_A2, Al,Ti;0) = -348892.407+280.179819*T$
		$MQ(BCC_A2, Ti,V) = -261912.01-157.174295*T$
	Ti	$MQ(BCC_A2, Al;0) = -104715.111-267.14*T$
		$MQ(BCC_A2, Ti;0) = -153362.077-126.135031*T$
		$MQ(BCC_A2, V;0) = -331128.104-65.0814985*T$
		$MQ(BCC_A2, Al,Ti;0) = -139719.202+294.400646*T$
		$MQ(BCC_A2, Ti,V;0) = +234932.489-219.426462*T$
	V	$MQ(BCC_A2, Ti,V;1) = -261099.972$
		$MQ(BCC_A2,Ti;0) = -179114.192-107.062681*T$
		$MQ(BCC_A2,V;0) = -322244.697-75.7262222*T$
		$MQ(BCC_A2,AL,Ti;0) = +421533.074-629.054528*T$
		$MQ(BCC_A2,Ti,V;0) = +163888.616-38.4124933*T$
HCP_A3	Al	$MQ(HCP,AL;0) = -131319-121.277*T$
		$MQ(HCP,Ti;0) = -311534.815-95.17706*T$
		$MQ(HCP,AL;0) = -111539.54-141.61855*T$
	Ti	$MQ(HCP,Ti;0) = -291755.355-115.51861*T$
		$MQ(HCP,V;0) = -298988.939-333.55846*T$
		$MQ(HCP,Ti;0) = -262867.416-95.5291479*T$
	V	$MQ(HCP,V;0) = -270101-313.569*T$
		$MQ(LIQUID,AL;0) = -26214.7168-129.362199*T$
		$MQ(LIQUID,Ti;0) = -66897.5497-125.188687*T$
	V	$MQ(LIQUID,V;0) = -354639.512$

Table 2. Excess Gibbs energies of alloys involved in this work [10]

Phase	Interaction parameter
BCC_A2	$L(BCC_A2,AL,V;0) = -136730+14.4*T$
	$L(BCC_A2,AL,V;1) = +131633-43*T$
	$L(BCC_A2,AL,Ti;0) = -132903+39.961*T$
	$L(BCC_A2,AL,Ti;1) = +4890$
	$L(BCC_A2,AL,Ti;2) = +400$
	$L(BCC_A2,AL,Ti,V;0) = +7315-100*T$
	$L(BCC_A2,AL,Ti,V;1) = -113926+40*T$
	$L(BCC_A2,AL,Ti,V;2) = +75972.5-150*T$
	$L(BCC_A2,Ti,V;0) = +6523.17$
	$L(BCC_A2,Ti,V;1) = +2025.39$
HCP_A3	$L(HCP,AL,Ti;0) = -134164+37.863*T$
	$L(HCP,AL,Ti;1) = -3475+.825*T$
	$L(HCP,AL,Ti;2) = -7756$
	$L(HCP,AL,Ti,V;0) = 0.0$
	$L(HCP,AL,Ti,V;1) = -206074-40*T$
	$L(HCP,AL,Ti,V;2) = 0.0$
LIQUID	$L(HCP,Ti,V;0) = +13233$
	$L(LIQUID,AL,V;0) = -122625.8+17.4*T$
	$L(LIQUID,AL,V;1) = +51463-.85*T$
	$L(LIQUID,AL,Ti;0) = (-154893+48.605*T)*EXP(-0.0002556*T)$
	$L(LIQUID,AL,Ti;1) = (-93896+74.406*T)*EXP(-0.0007032*T)$
	$L(LIQUID,AL,Ti;2) = (160157-3.4219*T)*EXP(-0.001641*T)$
	$L(LIQUID,AL,Ti,V;0) = -550000$
	$L(LIQUID,AL,Ti,V;1) = -50000$
	$L(LIQUID,AL,Ti,V;2) = +390000$
	$L(LIQUID,Ti,V;0) = +368.55$
	$L(LIQUID,Ti,V;1) = +2838.63$

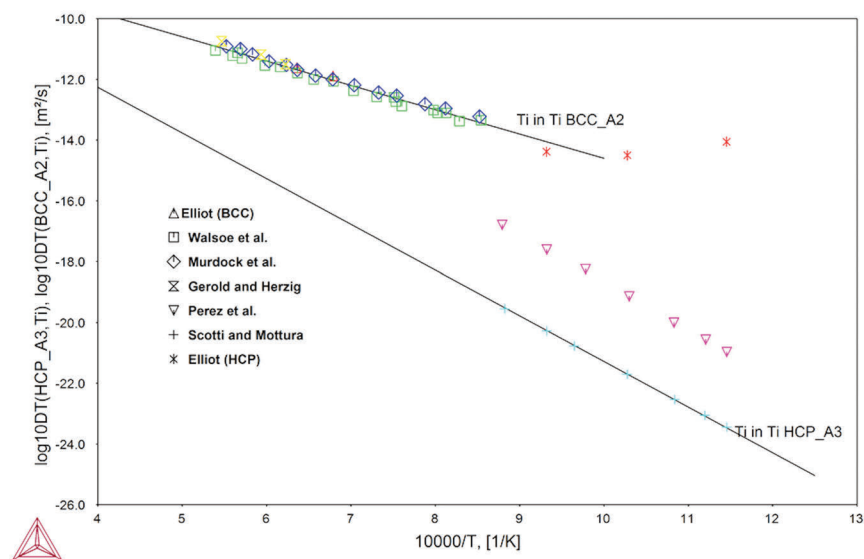


Figure 1. Self-diffusion of Ti in BCC_A2 and HCP_A3 phases superimposed with experimental data.

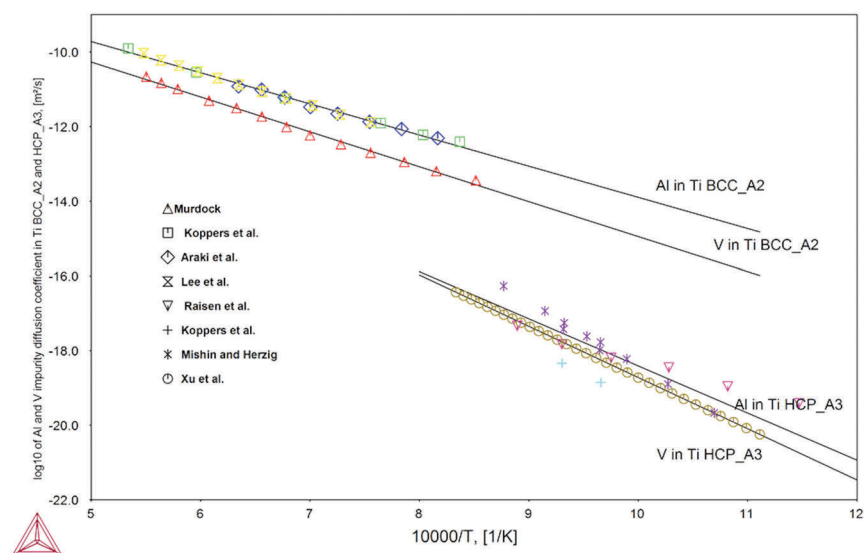


Figure 2. Impurity diffusion of Al in Ti – BCC and Ti – HCP together with experimental information.

optimization than data given by Scotti and Moutura [20] who presented self-diffusion of Ti in hexagonal structure in directions parallel and perpendicular to basal plane.

Calculated impurity diffusions of Al and Ti in pure Ti BCC_A2 as well as in pure Ti HCP together with available experimental data are shown in Figure 2. The impurity diffusion of aluminum in Ti BCC reproduces well experimental data. Moreover, it is easy to find out that all literature information [21-23] agrees with one another, therefore there was no problem with the modeling of this kinetic property. The impurity diffusion of vanadium in b-Ti was only

reported by Xu et al. [21] based on ab initio calculation. The impurity diffusion of aluminum in a-Ti reported by Raisen et al. [26] Koppers et al. [25] and Mishin and Herzig [27] show scattered character. During optimization of Al impurity diffusion coefficient in Ti HCP, all the data was given weight 1, consequently, the calculated impurity diffusion fits experiment with the best available accuracy. A bit different situation can be found in a case of vanadium impurity diffusion in pure Ti HCP. The only one experimental data was reported by Elliot [9]. One can see, that reported data is almost independent of temperature, what seems to be awkward. Thus, the

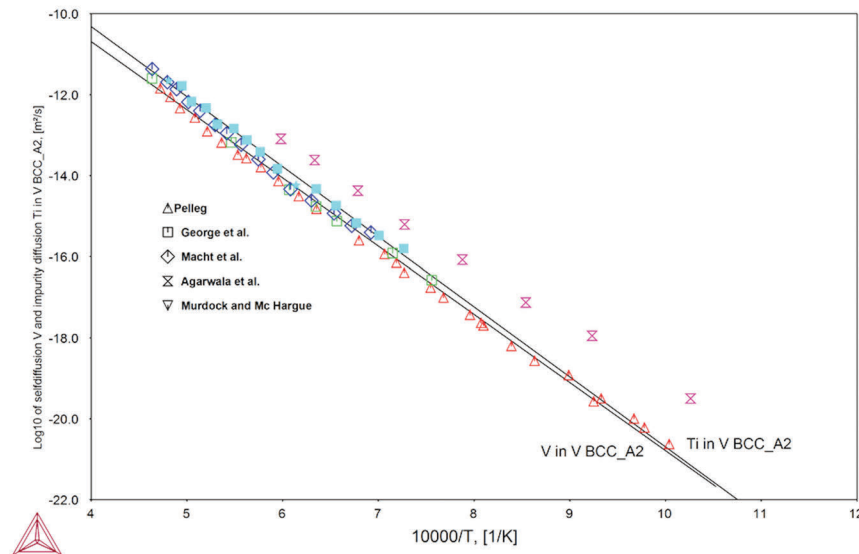


Figure 3. Self-diffusion of V in BCC_A2 and impurity diffusion of Ti in V-BCC superimposed experimental data.

calculated line was marked as dashed line and it can be written that more experimental data about V impurity diffusion in Ti HCP could improve the modeling and make it more trustable.

Figure 3 displays calculated self-diffusion of vanadium and impurity diffusion of titanium in pure V BCC_A2 phase superimposed with experimental data. The selfdiffusion V in V BCC_A2 in general agree with one another [15-17] except information given by Agarwala et al. [18] which reveals a quite different activation energy. Due to the situation, where three experimental datasets [15-17] give very similar data and

one dataset significantly varies [18], the last one was not included into calculation. The function obtained during optimization reproduces experimental information well and follows the data provided by Pelleg [15], George et al. [16] and Macht et al. [17]. The impurity diffusion of titanium in vanadium BCC_A2 was experimentally determined by Murdock and Mc Hargue [13]. The modeled function agrees well with experimental data. Using Figure 3, it can be concluded that diffusions of vanadium and titanium in V BCC_A2 show similar characteristic, i.e. similar activation energy and similar temperature dependency.

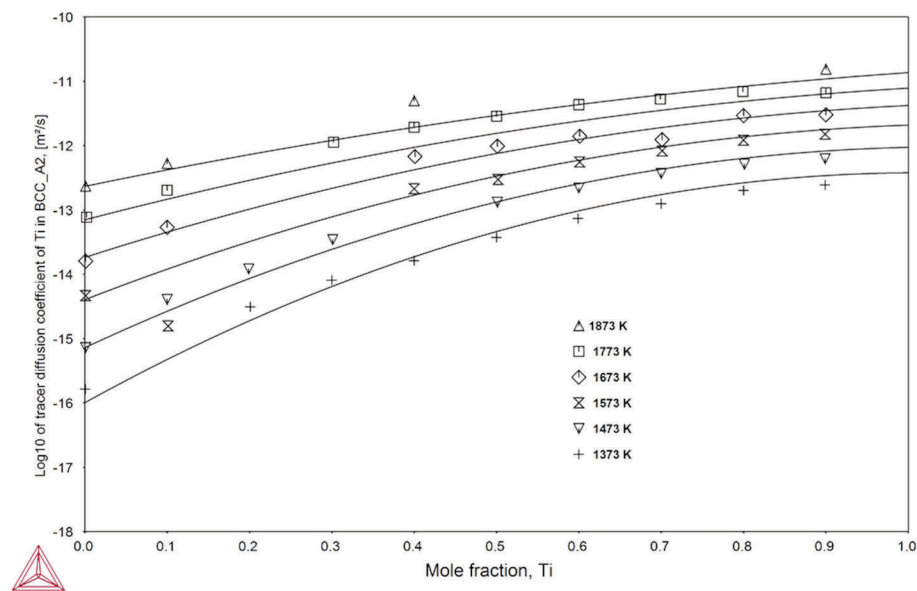


Figure 4. Ti tracer diffusion coefficient in Ti – V body centered cubic structure as function of temperature. In the same figure experimental data given by Murdock and McHargue [15] are placed.

The log 10 of Ti tracer diffusion coefficient in Ti-V BCC_A1 as a function of titanium compositions at temperature range 1473 K – 1873 K is shown in Figure 4 together with experimental data given by Murdock and McHargue [13]. It can be seen that experimental data is reproduced by calculation fair. At the first optimization step, the 0th degree parameter of Redlich-Kister polynomial was used and the obtained result was not satisfactory, therefore, a second term, with degree 1 was added to the description and after that the calculation showed much better agreement with the

data reported by Murdock and McHargue [13].

Figure 5 shows calculated log 10 of V tracer diffusion coefficient in Ti-V BCC_A2 phase for a full composition range at temperatures 1473 K, 1573 K, 1673 K, 1773 K, and 1873 K. In the same picture, experimental data given by Murdock and McHargue [13] is placed. It can be seen that the calculation and experimental data match pretty well and the discrepancy between calculated tracer diffusion of V and experiment is smaller than it was shown in a case of titanium tracer diffusion coefficient in Figure 4.

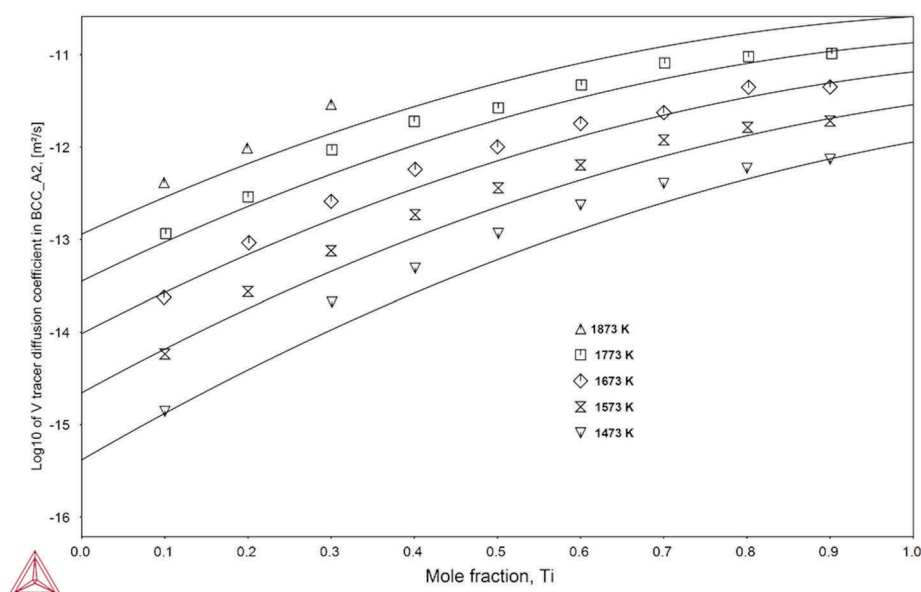


Figure 5. The logarithm of tracer diffusion coefficient in Ti – V BCC alloy as a function of temperature.

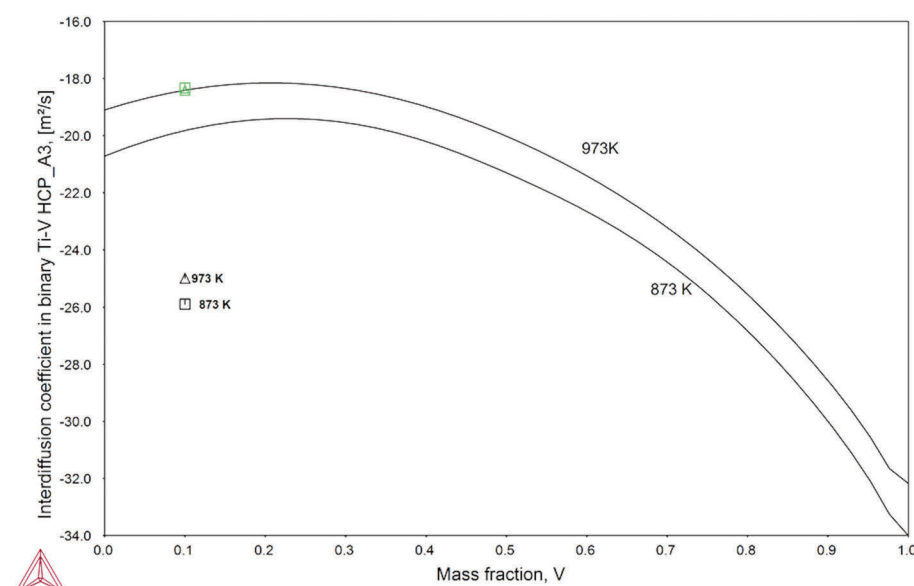


Figure 6. Interdiffusion coefficient in the binary Ti-V HCP phase.

To make calculation of interdiffusion in Ti-V binary HCP_A3 phase, the self-diffusion of V in a hypothetical V HCP_A3 structure was determined. To do it, the Leclair's [5] and Askil's [6] models, given by Equations 11 and 12, were used. The lattice constants were taken from ab initio calculations provided by Wang et al. [35], and the melting temperature of V in HCP_A3 was calculated from SGTE 5.1 database [36] as 1413.5 K. After applying the data to Equation 11 and 12, the self-diffusion of V in HCP_A3 was calculated. The obtained parameters are gathered in Table 1. Similarly, a diffusion of Ti in a hypothetical V HCP structure was calculated by a model proposed by Du et al. [7], which is described by Equations 13 and 14. The calculated values obtained from Equations 13 and 14 are also presented in Table 1. After these computations, it was possible to optimize interdiffusion coefficients based on experimental data given by Elliot [9]. Result of this optimization is shown in Figure 6.

It is obvious that calculation based on two experimental points should be treated as a very rough prediction only. The experimental data given by Elliot [9] shows no temperature dependency, when at the same time, the self-diffusion and impurity diffusion of Ti and V in binary Ti-V exhibit that dependency. Consequently, the calculation made at 973 K agrees with experimental data, and calculation made at 873 K shows a big difference between modeling and experiment. It seems to be reasonable result due to very awkward shape of interdiffusion function if calculation agree with experiment at both temperatures.

The obtained in this work interdiffusion

coefficient in binary Ti-Al BCC_A2 is shown in Figure 7.

In a case of interdiffusion modeling, the information about self-diffusion and impurity diffusion in a hypothetical Al BCC_A2 was necessary. The same procedure, as in a case of hypothetical HCP_A3 V, was applied to calculation of mobility parameters in hypothetical Al BCC_A2 and HCP_A3 structures, i.e. the semiempirical models given by Leclair [5] and Askil [6] were used for calculation of selfdiffusion of Al and model given by Du et al. [7] was used for calculation of interdiffusion. The crystal structure data for both atomic arrangements was taken from ab-initio calculation given by Wang et al [35]. The temperature of melting of Al in BCC_A2 and HCP_A3 was calculated at the first step from SGTE 5.1 database [36] but obtained result was not acceptable, i.e. the Gibbs energies of liquid Al and BCC_A2 Al didn't exhibit the same value for a reasonable temperature range. In the next step, the correction from ab initio modeling [31] was applied for calculation, and in this case the melting temperature of Al in BCC_A2 structure was equal 252 K, what also seemed to be too low. At the same time the melting temperature of Al in HCP_A3 structure was calculated as 802 K. To resolve this problem, an empirical model given by Boczkal [37,38] was used to estimate melting temperature of Al BCC_A2 and HCP_A3. The estimated temperatures were equal 761 K and 1069 for BCC_A2 and HCP_A3, respectively. For further calculations, the values obtained from Boczkal [37,38] for HCP_A3 and calculated from SGTE 5.1 database [36] corrected by ab initio [35] for BCC_A2 were used. Obtained values of mobility

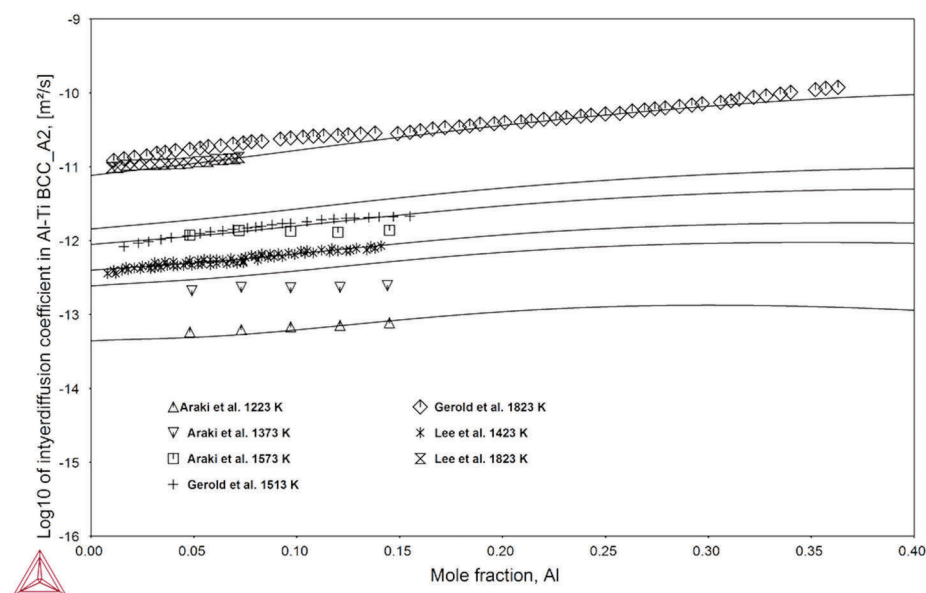


Figure 7. Interdiffusion coefficient in the binary Ti-Al BCC_A2.

parameters for hypothetical Al BCC_A2 and Al HCP_A3 are shown in Table 1.

The information about kinetic properties in ternary Al – Ti – V BCC_A2 are very limited, as it was written in a literature part. The ternary interaction parameters listed in Table 2 were obtained from data reported by Takahashi et al. [32] who provided values of impurity diffusion coefficients in ternary alloys as well as interdiffusion coefficients in ternary alloys at 1373 K and at 1473 K.

Figure 8 shows calculated impurity diffusion coefficient of V in Ti – Al BCC_A2 phase, as well as Al in Ti – V BCC_A2 as a function of concentration at 1573 L and 1373 K superimposed with data given by Takahashi et al. [32]. It is easy to see, that both interdiffusion coefficients agree pretty well with experimental data. Takahashi et al [32] also provided values of interdiffusion coefficients in ternary Al – Ti – V BCC_A2 alloy; however, due to

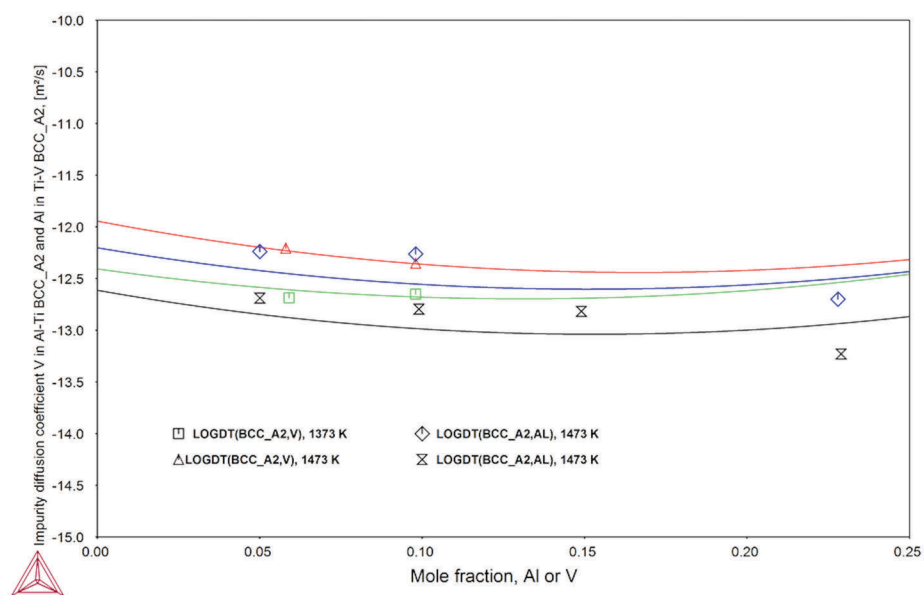


Figure 8. Impurity diffusion coefficient of V in Ti-Al and Al in Ti-V alloys at 1473 K and 1373 K superimposed with experimental data.

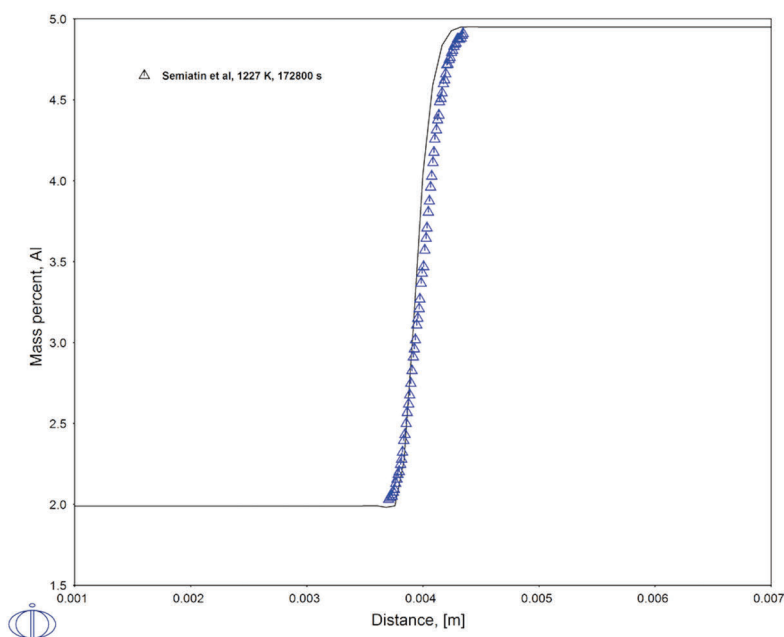


Figure 9. Simulation of diffusion couple Ti – 1.99 wt% Al – 7.48 wt% V / Ti – 4.95 wt% Al – 7.52 wt% V at 1227 K for 172800s superimposed with data given by Semiatin [32].

scattered compositions of experiment it was impossible to show a graphical representation of this data because calculation has to be made along a path where a composition is given as a function or constant.

Calculated Al concentration profile in diffusion couple Ti – 1.99 wt% Al – 7.48 wt% V / Ti – 4.95 wt% Al – 7.52 wt% V superimposed with experimental data given by Semiati et al. [33] is displayed in Figure 9. Simulation and experiment were done at temperature 1227 K and homogenization time was set as 172,800 second (48h). The reader can see that simulation follows experimental data pretty well, with only a small discrepancy at high concentration of aluminum. Therefore, it can be concluded that proposed kinetic description of the BCC_A2 phase can be used for modeling of atomic mobility in this phase.

The precipitation of HCP_A 3 phase was simulated using Prisma module of the ThermoCalc [34] software. For this simulation, the initial concentration of BCC_A2 phase was set as $x_V = 0.036$, and $x_{Al} = 0.1019$ at 1173 K. The molar volume of alloy in BCC_A2 and HCP_A3 structures were calculated as superposition of molar volumes of pure elements due to very small amount of Al and V in the alloy. The obtained values were equal $1.08726E-05$ and $1.08663E-05$ m³/mole for HCP_A3 and BCC_A2 structure, respectively [39]. The mobility of HCP_A3

phase boundary was assumed to be 10 m⁴/Js. The result of simulation is shown in Figure 10. As same as the result of diffusion couple simulation, also calculation of precipitation is in a great interest of application. Changing parameters of simulation (time, temperature, morphology of precipitated phase) one can predict a heat treatment of such important alloys as Titanium grade 5. Moreover, the proposed kinetic database can find application during description of higher-ordered systems, such as Ti-2.7Al-5.7Fe-6Mo-6V [40].

6. Summary

The mobility of Ti, Al, and V in Titanium grade 5 was optimized based on available experimental information and empirical approaches. The description of kinetic properties of liquid, BCC_A2 and HCP_A3 phases was proposed. Comparison between simulations and experiments shows a good agreement, therefore it can be concluded that suggested set of mobility parameters can be used for prediction of diffusion couple behavior, homogenization, or heat treatment.

Acknowledgments

The work was supported by Ministry of Science and Technology (Taiwan) under grant no. 107-2221-E-259 -011.

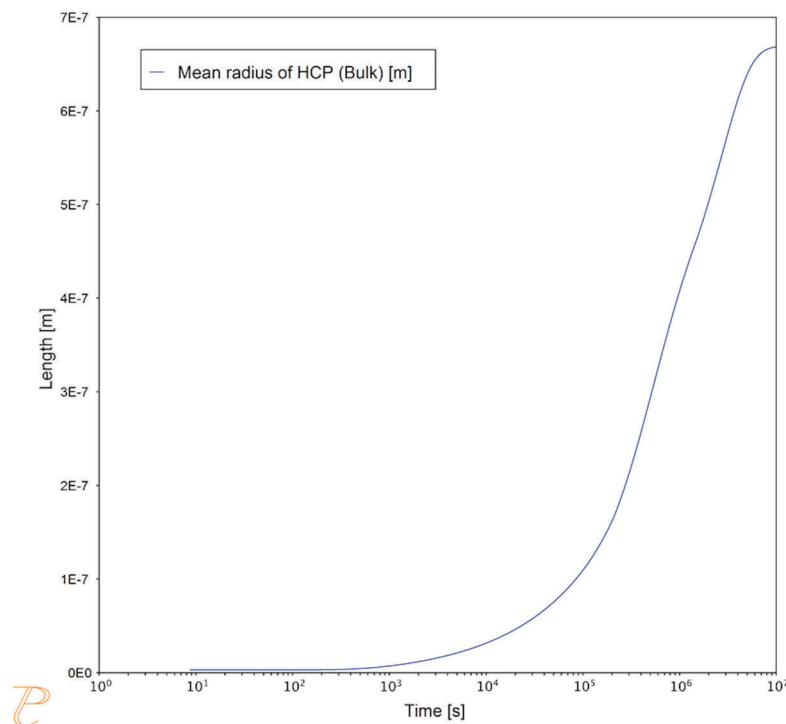


Figure 10. Simulation of precipitation of HCP_A3 phase from BCC_A2 phase at 1173 K

Appendix 1. Thermodynamic re-optimization of Ti-Al liquid phase

The thermodynamic description of Ti-Al system provided by Witusiewicz et al. [41] and adopted in [10] exhibits an inverted miscibility gap in liquid phase at high temperatures as it is shown in Figure A1.

It is obvious that an inverted miscibility gap is an artifact produced by the model, not the real behavior of a liquid phase. Therefore, it was decided to re-optimize the liquid phase keeping thermodynamic description of all liquid phases. In this procedure, the following experimental data were used: activity of Al in liquid phase specified by Maeda et al. [42], enthalpy of mixing of liquid phase reported by Esin et al. [43, 44], invariant reactions provided by Hall and Huang [45], Yu et al. [46], Ence and Margolin [47], Bulanova et al. [48], McPherson and Hansen [49], Snow et al. [50], as well as liquidus and solidus data described by Kornilov et al. [51], Perepezko et al. [52], Fink et al. [53], Manchot and Leber [54], Erckelens [55] and Schuster and Ipser [56].

Since the linear model [57] produced inverted miscibility gap it was decided to use an exponential model, proposed by Kaptay [58]. In this model, the interaction parameters jL are given as follows:

$${}^jL_{Al,Ti}^{Liquid} = {}^j h_{Al,Ti}^{Liquid} \cdot \exp\left(-\frac{T}{{}^j \tau_{Al,Ti}^{Liquid}}\right) \quad (A1)$$

Where ${}^jL_{Al,Ti}^{Liquid}$ is an interaction parameter of J-th degree, ${}^j h_{Al,Ti}^{Liquid}$ is the enthalpy part of the interaction energy, ${}^j \tau_{Al,Ti}^{Liquid}$ is a special temperature, at which the interaction energy would cross zero if it was described by the linear model, T is the absolute temperature.

Unfortunately, this approach produced artifact at low temperature, i.e. the liquid stable became stable from 0K up to 350 K for concentration of Al equal; c.a. 0.35 mole fraction. This kind of artifact was also shown by Schmid -Fetzer et al. [59]; however, it has to be emphasized that in their case [59], as well as for this study, the full optimization was not run. To resolve this problem, the combined linear-exponential model [60] was used for optimization of the liquid phase in Al – Ti system. In this model, the interaction parameter is given by Equation A2:

$${}^jL_{Al,Ti}^{Liquid} = ({}^j h_{Al,Ti}^{Liquid} - {}^j s_{Al,Ti}^{Liquid} T) \cdot \exp\left(-\frac{T}{{}^j \tau_{Al,Ti}^{Liquid}}\right) \quad (A2)$$

Where ${}^j s_{Al,Ti}^{Liquid}$ is the entropy part of the interaction energy.

After applying Eq. A2 the optimization of the liquid phase was performed and a new description of Gibbs energy of the binary liquid Al – Ti was obtained. Next, the phase diagram and thermodynamic functions were calculated and compared with available experimental data. Figure A2 shows calculated phase diagram of the Ti – Al system. One can see that the inverted miscibility gap is not

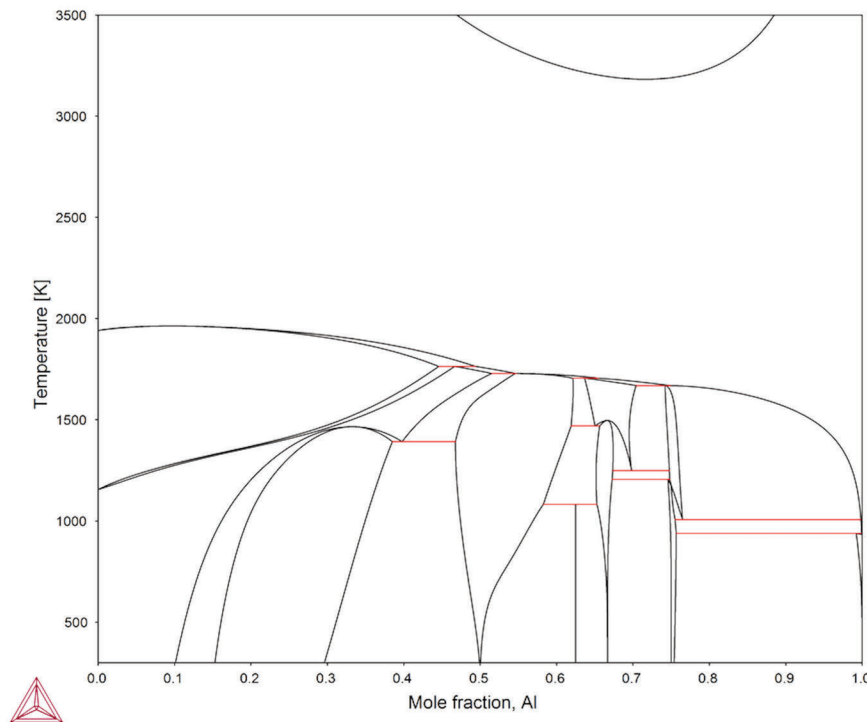


Figure A1. Calculated phase diagram based on Witusiewicz et al [A1] description. The reader can see inverted miscibility gab in the liquid phase at high temperature.

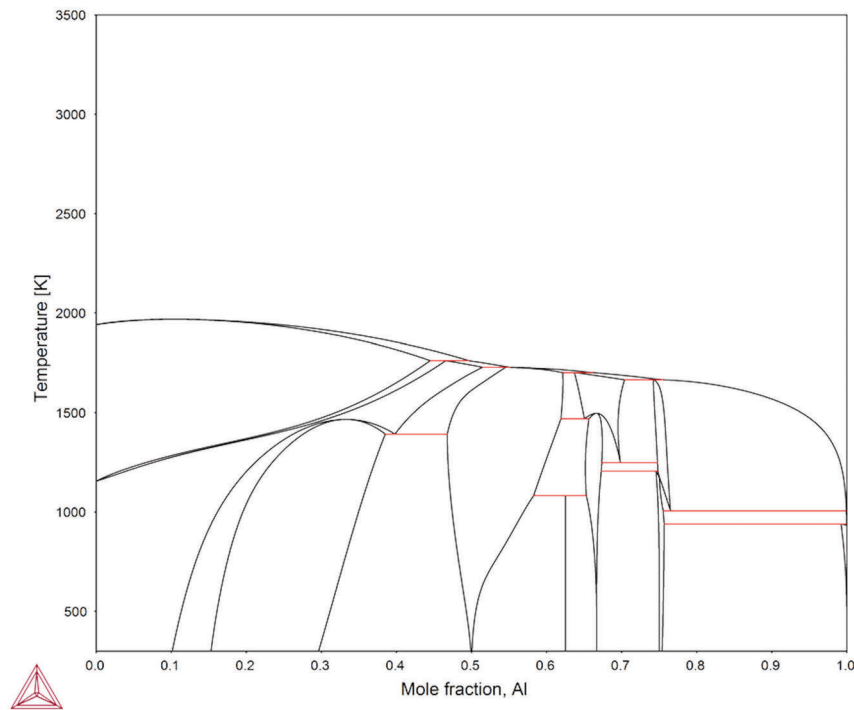


Figure A2. Calculated phase diagram after re-optimization of liquid phase.
The inverted miscibility gap is not provided at high temperature.

presented in the proposed description of the liquid phase. The final values of parameters obtained in this work are gathered in Table 2 in the main part of this paper.

References

- [1] J. Liu, S. Suslov, S. Li, H. Qin, Z. Ren, C. Ma, G. X. Wang, G. L. Doll, H. Cong, Y. Dong, C. Ye, *Surf. Coat. Technol.* 325 (2017) 289–298.
- [2] W. Liu, Y. Lin, Y. Chen, T. Shi, S. Ambrish, *Rare Met. Mater.* 46 (2017) 634 – 639.
- [3] J. O. Andersson, J. Ågren, *J. Appl. Phys.* 72 (1992) 1350 - 1355.
- [4] A. Redlich, A. Kister, *Ind. Eng. Chem.* 40 (1948) 345 – 348.
- [5] A. D. Leclair, *Phil. Mag.* 7 (1962) 141 – 167.
- [6] J. Askill, *Alloys and Simple Oxides*, IFI Plenum, 1970.
- [7] Y. Du, W.B. Zhang, D.D. Liu, S.L. Cui, D.D. Zhao, L.J. Zhang, H.H. Xu, NIST 2010 Diffusion Workshop, March 23–24 2010, Maryland, USA
- [8] H. Fredriksson, U. Akerlind, *Physics of Functional Materials*, J. Wiley & Sons, Ltd. UK 2008.
- [9] R. P. Elliot, Technical Documentary Report No. AST-TDR-62-561, Armed Service Technical Information Agency, Arlington Hall Station, Arlington 12, Virginia, USA, 1962.
- [10] J. Murdock, T. Lundy, E. Stansbury, *Acta Metall.* 12 (1964) 1033–1039.
- [11] U. Gerold, C. Herzig, *Def. Diff. Forum* 143–147 (1997) 437–442.
- [12] N. Walsoe, D. Reza, C. Libanati, *Acta Metall.* 16 (1968) 1297–1305.
- [13] J. Murdock, C. McHargue, *Acta Metall.* 16 (1968) 493–500.
- [14] Y. Ugaste, Y. Zaykin, *Fiz. Metal. I Metalloved* 40 (3) (1975) 567–575.
- [15] J. Pelleg, *Phil. Mag.* 29 (2) (1974) 383–393.
- [16] B. George, C. Janot, D. Ablitzer, Y. Chabre, *Phil. Mag. A* 44 (1981) 763–778.
- [17] M. Macht, G. Froberg, H. Wever, *Z. Metallkd.* 70 (1979) 209–214.
- [18] R. Agarwala, S. Murarka, M. Anand, *Acta Metall.* 16 (1968) 61–67.
- [19] R. A. Perez, H. Nakajima, F. Dymont, *Materials Trans.* 44 (2003) 2 – 13.
- [20] L. Scotti, A. Mottura, *J. Chem. Phys.* 142 (2015) 204 – 308
- [21] W. Xu, S. L. Shang, C. C. Zhou, X. Liu, C. Wang, Z. K. Liu, NIST Materials Data Repository <https://materialsdata.nist.gov/handle/11256/619> retrieved on 2017-11-27.
- [22] M. Koppers, C. Herzig, M. Friesel, Y. Mishin, *Acta Mater.* 45 (1997) 4181 – 4191 .
- [23] H. Araki, T. Yamane, Y. Minamino, S. Saji, Y. Hana, S. B. Jung, *Metall. Mater. Trans.* 25 A (1994) 874 – 876.
- [24] S. Y. Lee, O. Taguchi, Y. Iijima, *Materials Trans.* 51 (2010) 1809–1813.
- [25] M. Koppers, D. Derau, M. Fries, C. Herzig, *Defect. Diffusi. Forum.*, 143–1467(1997) 43–48.
- [26] J. Raisen, A. Anttila, J. Keinonen, *J. Appl. Phys.* A 86(4) (2006) 481–484

- [27] Y. Mishin, C. Herzig, *Acta Mater.* 48 (2000) 589-623.
- [28] R. Kainuma, G. Inden, Z. Metallkd. 88 (1997) 428 – 432.
- [29] X. Lu, N. Gui, A. Qiu, C. H. Li, *Mater. Trans.A* 45(9) (2014) 4155 – 4164.
- [30] Y. Liu, Y. Ge, D. Yu, T. Pan, L. Zhang, J. All. Comp. 470 (2009) 176-182.
- [31] Y. Chen, J. Li, B. Tang, H. Kou, J. Seguardo, Y. Cui, *CALPHAD* 46 (2014) 205-212.
- [32] T. Takahashi, Y. Minamino, M. Komatsu, *Mater. Trans.*, 49 (2008) 125-132.
- [33] S. I. Siemiatin, T. M. Brown, T. A. Goff, P. N. Fagin, D. R. Barker, R. E. Turner, J. M. Murry, J. D. Miller, F. Zhang, *Mater. Trans. A*, 35 A (2004) 3015 – 3018.
- [34] J. O. Andersson, T. Helander, L. Höglund, P. F. Shi, B. Sundman, *Calphad* 26 (2002) 273-312.
- [35] Y. Wang, S. Curtarolo, C. Jiang, R. Arroyave, T. Wang, G. Ceder, L.-Q. Chen, Z.-K. Liu, *Calphad* 28 (2004) 79-90.
- [36] SGTE 5.1 Database, Scientific Group ThermoData Europe 2014.
- [37] G. Boczkal, *Arch. Metall. Mater.* 60 (2015) 2457 – 2460.
- [38] G. Boczkal, *Mater. Lett.* 134 (2014) 162 – 264.
- [39] J. Yan, *TRIP Titanium Alloy Design*, PhD Thesis, Northwestern University, USA, 2014.
- [40] T. D. Mytava, L. A. Cornish, I. Sigalas, J. Min. Metall. Sect. B-Metall. 53 (3) B (2017) 263-270.
- [41] V. T. Witusiewicz, A. A. Bondar, U. Hecht, S. Rex, T. Y. Velikanova, J. All. Comp. 465 (2008) 64-67.
- [42] M. Maeda, T. Kiwake, K. Shibuya, T. Ikeda, *Mat. Sci. Eng. A* 239-240 (1997) 276-280.
- [43] Yu.O. Esin, N.P. Bobrov, M.S. Petrushevskiy, P.V. Gel'd, *Izv. Akad.Nauk SSR, Met.* 5 (1974) 104–109 (in Russian).
- [44] Yu.O. Esin, N.P. Bobrov, M.S. Petrushevskii, P.V. Gel'd, *Tep. Vys. Temp.* 13 (1975) 84–88 (in Russian).
- [45] E.L. Hall, S.C. Huang, *Acta Metall. Mater.* 38 (1990) 539–549.
- [46] Yu. Kovneristy, P.B. Budberg, in: I.V. Gorynin, S.S. Ushkov (Eds.), *Titanium'99—Science and Technology*, vol.1 1, Prometey, 2000, St. Petersburg, Russia, 115–123.
- [47] A7. E. Ence, H. Margolin, *Trans. Metall. Soc. AIME* 221 (1961) 151–157.
- [48] M. Bulanova, L. Tretyachenko, M. Golovkova, K. Meleshevich, *J. Phase Equilib.* 25 (2004) 209–229.
- [49] D.J. McPherson, M. Hansen, *Z. Metallkd.* 45 (1954) 76–82 (in German).
- [50] D.B. Snow, C.T. Burilla, B.F. Oliver, in: F.H. Froes, I. Caplan (Eds.), *Titanium'92—Science and Technology*, vol. 2, TMS, 1993, USA, 1091–1098.
- [51] I.I. Kornilov, E.N. Pylaeva, M.A. Volkova, *Izv. Akad. Nauk. SSSR, Otd. Khim. Nauk* 7 (1956) 771–778 (in Russian).
- [52] J.H. Perepezko, J.C. Mishurda, in: F.H. Froes, I. Caplan (Eds.), *Titanium'92—Science and Technology*, vol. 1, TMS, 1993, USA, 563–570.
- [53] W.L. Fink, K.R. van Horn, P.M. Budge, *Trans. AIME* 93 (1931) 421–439.
- [54] W. Manchot, A. Leber, *Z. Anorg. Allg. Chem.* 150 (1926) 26–34 (in German).
- [55] E. van Erckelens, *Metall. Erz* 20 (11) (1923) 206–210 (in German).
- [56] J.C. Schuster, H. Ipser, *Z. Metallkd.* 81 (1990) 389–396 (in German).
- [57] H. L. Lukas, S. G. Fries, B. Sundman, *Computational Thermodynamics. The Calphad Method*. Cambridge University Press, Cambridge, UK, 2007.
- [58] G. Kaptay, *Calphad* 20 (2004) 115-124.
- [59] R. Schmid-Fetzer, D. Anderson, P. Y. Chevalier, L. Eleno, O. Fabrichnaya, U. R. Kattner, B. Sundman, C. Wang, A. Watson, L. Zabdyr, M. Zinchievich, *Calphad* 31 (2007) 38-52.
- [60] G. Kaptay, *Calphad* 56 (2017) 169-184.

POKRETLJIVOST ATOMA U LEGURI TITANIJUMA GRADE 5 (Ti6Al4V)

W. Gierlotka ^a, G. Lothongkum ^b, B. Lohwongwatana ^b, C. Puncreoburt ^b

^a Odsek za nauku o materijalima i inženjerstvo, Nacionalni tajvanski univerzitet, Tajvan, Republika Kina

^b Odsek za metalurško inženjerstvo, Univerzitet Čulalongkorn, Tajland

Apstrakt

Titanijum grade 5 (Ti6Al4V) je savremeni materijal koji ima široku primenu u oblastima kao što su medicina do primene u avio industriji. Komercijalna legura predstavlja mešavinu prostorno centrirane kubne strukture (BCC_A2) i heksagonalno gusto pakovane strukture (HCP_A3). Očigledno je da toplotna obrada legure menja odnos između BCC_A2 i HCP_A3, a kao posledica postupka, menjaju se i osobine materijala. Podaci o pokretljivosti atoma u obe kristalne strukture omogućavaju simulacije i predviđanje ponašanja prilikom toplotne obrade i difuzije. U ovom radu je ispitivana pokretljivost atoma u tečnoj fazi, kao i u BCC_A2 i HCP_A3 fazama trojne legure Al – Ti – V, a na osnovu podataka iz dostupne literature. Poređenja između rezultata simulacija i eksperimenata pokazuju da se oni podudaraju, te se stoga može doći do zaključka da se predloženi skup kinetičkih parametara može koristiti za predviđanja i simulacije termičke obrade legure titanijuma grade 5.

Ključne reči: Titanijum; Kinetičko modelovanje; DICTRA.

